Engineering of three-dimensional pre-vascular networks within fibrin hydrogel constructs by microfluidic control over reciprocal cell signaling

Barbara Bachmann,[1,2,3,4,a)] Sarah Spitz,[1,4,5,a)] Mario Rothbauer,[1,a)] Christian Jordan,[1] Michaela Purtscher,[6] Helene Zirath,[1] Patrick Schuller,[1] Christoph Eilenberger,[1] Syed Faheem Ali,[1,3,4] Severin Mühleder,[2,3,4] Eleni Priglinger,[2,4] Michael Harasek,[1] Heinz Redl,[2,3,4,5] Wolfgang Holnthoner,[2,3,4] and Peter Ertl[1,3,4,b)]

[1]*Faculty of Technical Chemistry, Institute of Applied Synthetic Chemistry, Institute of Chemical Technologies and Analytics, Vienna University of Technology, 1060 Vienna, Austria*
[2]*AUVA Research Centre, Ludwig Boltzmann Institute for Experimental and Clinical Traumatology, 1200 Vienna, Austria*
[3]*Kompetenzzentrum für MechanoBiologie (INTERREG V-A AT-CZ ATCZ133), 1200 Vienna, Austria*
[4]*Austrian Cluster for Tissue Regeneration, 1200 Vienna, Austria*
[5]*Trauma Care Consult GmbH, Vienna, 1200 Vienna, Austria*
[6]*Department of Biochemical Engineering, University of Applied Sciences Technikum Wien, 1060 Vienna, Austria*

(Received 27 February 2018; accepted 6 June 2018; published online 20 June 2018)

Reengineering functional vascular networks *in vitro* remains an integral part in tissue engineering, since the incorporation of non-perfused tissues results in restricted nutrient supply and limited waste removal. Microfluidic devices are routinely used to mimic both physiological and pathological vascular microenvironments. Current procedures either involve the investigation of growth factor gradients and interstitial flow on endothelial cell sprouting alone or on the heterotypic cell-cell interactions between endothelial and mural cells. However, limited research has been conducted on the influence of flow on co-cultures of these cells. Here, we exploited the ability of microfluidics to create and monitor spatiotemporal gradients to investigate the influence of growth factor supply and elution on vascularization using static as well as indirect and direct flow setups. Co-cultures of human adipose-derived stem/stromal cells and human umbilical vein endothelial cells embedded in fibrin hydrogels were found to be severely affected by diffusion limited growth factor gradients as well as by elution of reciprocal signaling molecules during both static and flow conditions. Static cultures formed pre-vascular networks up to a depth of 4 mm into the construct with subsequent decline due to diffusion limitation. In contrast, indirect flow conditions enhanced endothelial cell sprouting but failed to form vascular networks. Additionally, complete inhibition of pre-vascular network formation was observable for direct application of flow through the hydrogel with decline of endothelial cell viability after seven days. Using finite volume CFD simulations of different sized molecules vital for pre-vascular network formation into and out of the hydrogel constructs, we found that interstitial flow enhances growth factor supply to the cells in the bulk of the chamber but elutes cellular secretome, resulting in truncated, premature vascularization. *Published by AIP Publishing.* https://doi.org/10.1063/1.5027054

[a)]B. Bachmann, S. Spitz, and M. Rothbauer contributed equally to this work.
[b)]Author to whom correspondence should be addressed: peter.ertl@tuwien.ac.at

INTRODUCTION

A major issue in tissue engineering is the formation of necrotic cores inside biological structures due to limited diffusion of oxygen and nutrients to tissue regions beyond 200–400 μm. One promising strategy to overcome apparent oxygen and nutrient deficiencies is based on the integration of lumenized and perfused vessels to promote long-term viability of tissue-engineered constructs.[1] Over the last decade, generation of vascularized tissues has steadily improved enabling controlled nutrient supply and waste removal to and from the engineered construct through blood vessel-like networks.[2,3] From a physiological point of view, blood vessels are generally formed by two distinct mechanisms being vasculo- and angiogenesis.[4] While vasculogenesis refers to the *de novo* formation of blood vessels during embryonic development, angiogenesis requires a pre-existing vasculature, which can be extended by sprouting endothelial cells.[5] Additionally, mural cells such as vascular smooth muscle cells and pericytes actively take part in vessel maturation and stabilization.[6] While smooth muscle cells form concentric layers around arteries and veins, pericytes partially envelope smaller sized structures including arterioles, capillaries, and venules.[7] Coordination of endothelial cell sprouting is therefore guided by both reciprocal cell signaling events and heterotypic cell-to-cell contact. Similar sprouting behavior has also been observed in the presence of adipose and bone-marrow derived mesenchymal stem cells, which are known to mimic mural cells through heterotypic cell-cell interactions with endothelial cells.[6,8,9] Mesenchymal stem cells secrete numerous factors including vascular-endothelial growth factor (VEGF) and hepatocyte growth factor (HGF) that not only contribute to endothelial cell survival and proliferation but also promote the formation of pre-vascular structures *in vitro*.[8,10,11] Although the importance of reciprocal cell signaling on endothelial cell sprouting has been extensively studied over the years,[6] little is still known on the influence of growth factor gradients, which are inherently present in any natural and engineered tissue construct.

To gain a deeper understanding of the modulating effect of spatio-temporal gradients on the formation of pre-vascular networks, we have developed three different microfluidic devices that allow precise control over nutrient supply from predefined entry points to a 3D-hydrogel based co-culture system. Microfluidic cell culture systems are ideally suited to study vascular biology due to the inherent ability to control the respective microenvironment.[12–17] For instance, 2D microfluidic endothelial cell cultures systems have been used to elucidate the impact of growth factor gradients in intra- and extravasation of cancer cells[18–20] as well as VEGF[21,22] and angiopoietin-1 (ANG-1) gradients in endothelial cell sprouting.[21] In addition to demonstrating the importance of VEGF gradients for the formation of blood vessels,[23,24] microfluidic devices are routinely employed to provide physiologically relevant shear and interstitial flow regimes.[25] As an example, changes in endothelial cell morphology, phenotype, and proliferative capacity have been reported for increasing shear conditions ranging up to 130 dyn cm^{-2}.[26] While under physiological shear stress of 0.1 dyn cm^{-2} to 3 dyn cm^{-2}, a decrease in endothelial sprouting has been reported,[23] shear restriction and the presence of interstitial flow velocities between 1 μm/s and 35 μm s^{-1}, in turn, have shown to positively affect vasculo- and angiogenesis.[23,27,28] Although, in the absence of supporting cells, these microfluidic endothelial cell culture systems failed to recapitulate the physiological architecture of microvessels in interstitial tissues, these studies still demonstrated that growth factor gradients may influence sprouting. Interestingly, all existing perfused microvascular networks based on co-culture of endothelial cells and mural cells did not consider apparent wash out effects and gradients of soluble growth factors during interstitial flow conditions.[20,29,30] While current microfluidic strategies mainly focus on engineering perfusable vascular networks in tumor models[20,31] and investigating endothelial barrier functions,[32] we aim at utilizing microfluidics to fine tune vascular network formation by controlling growth factor gradients and flow profiles. In contrast to previously reported vascularization on chip models, which focus on perfusable networks anastomosed to the microfluidic channel, the goal of this study is to establish enlarged tissue constructs for potential applications in tissue engineering. This means that our microfluidic

chamber geometries greatly vary from previously published vasculature-on-chip work in terms of chamber size as well as hydrogel boundary surface.

To close this knowledge gap and to gain a deeper understanding of the relationship between heterotypic cell-to-cell interactions and reciprocal cell signaling during initial endothelial cell sprouting, a dual *in vitro* and *in silico* strategy is employed to describe the effects of spatial depletion of growth factors on the formation of a vascular network. In our experimental approach, three microfluidic 3D co-culture systems, which contain adipose-derived stem cells as supporting cells and human umbilical vein endothelial cells embedded in a fibrin matrix, are used to evaluate vascular network area coverage and average microvessel length over a seven day cultivation period. Similar to recent publications in the field,[25,31] an initial vascular network formed after five days of culture with a mature vascular network after seven days. The microfluidic biochips are designed either for indirect and lateral perfusion or direct flow conditions to establish various gradients in 1, 3, and 8 mm thick 3D vascular co-culture systems. Additional finite volume CFD simulations are performed to characterize transport phenomena and distance-relationships of signaling molecules and growth factors of increasing sizes ranging from 10 kDa, 20 kDa, 40 kDa, to 500 kDa in the absence and presence of varying interstitial flow conditions. Since the individual and combinatorial biophysical constraints such as interstitial flow, size-dependent gradients, and tissue dimension are keys in vascular network formation, a better understanding of their modulating effects may provide new insight into angiogenesis, tissue regeneration, and cancer biology.

MATERIALS AND METHODS

Device fabrication

Three microfluidic devices were used for characterization of tube formation under static or fluid flow conditions. Two of the devices had a circular chamber adjacent to a medium channel (see Fig. 1 and supplementary material Fig. 1). Microstructures were fabricated using polydimethylsiloxane (PDMS, Sylgard® 184 Silicone Elastomer Kit, Down Corning) by soft lithography from 3D-printed molds (i.materialise). After polymerization, the PDMS was bonded to glass slides using air plasma (Harrick Plasma, High Power, 2 min) and sterilized with 70% ethanol

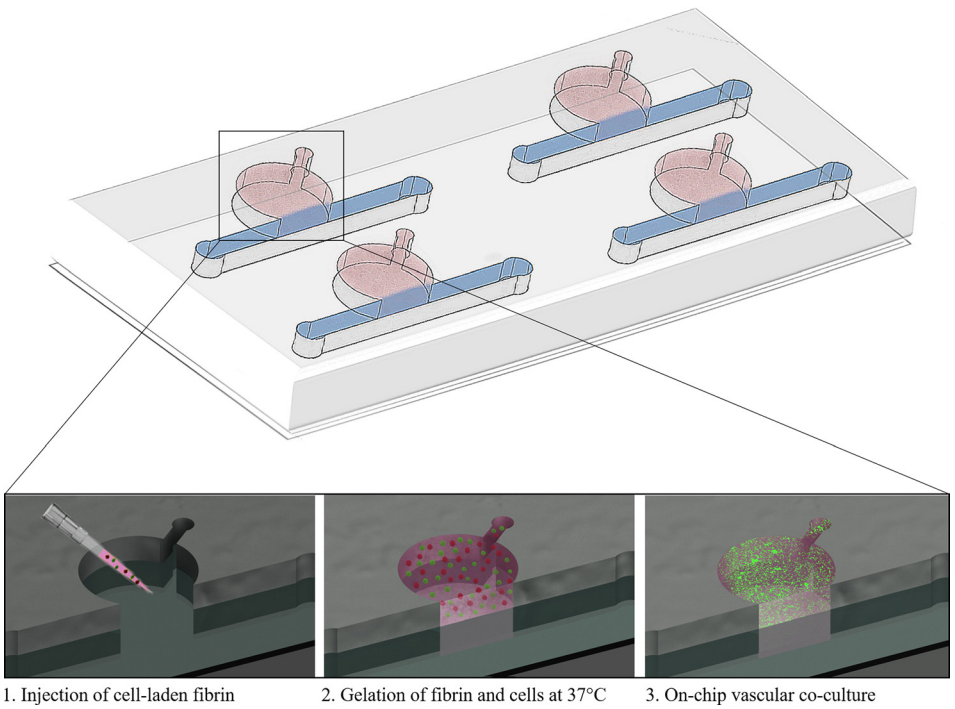

FIG. 1. Schematic overview of the microfluidic device and cell loading procedure.

before use. In turn, the microfluidic biochip designed for direct perfusion through hydrogel [see Fig. 4(a)] was manufactured using a PDMS-sheet cutter (CAMM-1 GS-24, Roland DGA). After cutting the microchannel network into PDMS membranes, the fluidic layer was sandwiched between two glass slides, sealed via air plasma activation, and treated with 3% (3-Aminopropyl) triethoxysilane (APTES; Sigma Aldrich) solution for 1 h. The assembled microfluidic biochips were sterilized (70% ethanol), rinsed with de-ionized (DI) water for a period of 30 min, and coated with 10 mg/ml fibrinogen solution overnight.

Cell culture and device seeding

Isolation of human adipose-derived stem cells (ASC) as well as human umbilical vein endothelial cells (HUVEC) was carried out as previously described[33,34] following the approval of the ethics committees (state of Upper Austria and the AUVA) and written donor consent. Harvested cells were maintained in fully supplemented endothelial cell growth medium 2 (EGM-2, PromoCell) with 5% fetal calf serum until passage 5 to 9. Retroviral infection of GFP-HUVECs was carried out as previously published.[35,36] Prior to cell seeding into microfluidic devices, fibrin hydrogel (TISSEEL®, Baxter) with a final concentrations of 2.5 mg/ml fibrinogen, 1 U/ml thrombin, and 5×10^5 cells/ml per cell type was loaded into the hydrogel chambers and polymerized for 45 min. Cell cultivation was carried out in the presence of fully supplemented EGM-2 medium under static conditions (exchange of medium every other day) and constant perfusion over a period of 7 days with four replicas per condition. Adipose-derived stem cell conditioned medium was generated by seeding 3500 cells/cm^2 and collecting secretome after three days of incubation. Non-treated controls were similarly incubated in culture flasks without cells. For experiments using a temporal adjustment of flow, co-cultures were statically cultivated for three days before initiation of flow using fresh culture medium for five days.

Finite volume CFD simulation

A multipurpose finite volume CFD code was used for solving the flow problems. The geometries were split in hexahedral control volumes, an example grid is presented in supplementary Fig. 2A. Second or higher order discretization was selected for all flow variables as well as for the species equations. To ensure physically correct transient solutions, the time step size was selected to guarantee a maximum Courant number $\mathrm{Co} < 1$ within the flow domain over the whole run time of up to 18 h. Wall boundaries were treated as ideally smooth, no slip boundary conditions were selected for all surfaces. The inlet of the flow geometry was set to mass flow inlet with a plug flow velocity profile, and the outlet was set to pressure outlet at a standard pressure of 1 atm (101325 Pa) with the flow considered to be isothermal. For simplicity, Newtonian fluid behavior was assumed with a constant dynamic viscosity and constant density. As the concentrations of the dissolved species in the fluid are low, the properties of the solvent, water, have been used for the simulation ($\rho = 998\,\mathrm{kg/m^3}$, $\eta = 0.001003\,\mathrm{Pa\ s}$). The diffusion coefficients for the tracer components have been set according to measurements or literature values, assuming a dilute solution. Tracers at the flow inlet were added as step functions at the initial time $\mathrm{T} = 0$ s, and at the same time a constant tracer saturation of the hydrogel zones were set as starting values for the simulation runs. In addition to the tracer species, a non-diffusing scalar was tracked for calculation of the residence time distributions—an example can be found in S1B. The maximum Reynolds number Re within the geometry was $\ll 1$; therefore, laminar flow was assumed with no boundary layer grid. The hydrogel regions were approximated as porous zones with constant porosities of $\varepsilon = 0.99$ and isotropic viscous resistances of $\mathrm{R} = 6.67 \times 10^{-12}\ \mathrm{m^{-2}}$.

Data analysis

All microfluidic devices were analyzed on day 7 based on green fluorescence intensities obtained from transfected HUVECs using AngioTool64 software [Version 0.6a (02.18.14)] to determine network parameters as described elsewhere.[37]

RESULTS AND DISCUSSION

Impact of hydrogel volume and diffusion distances on reciprocal signaling during pre-vascular network formation

Microfluidic devices similar in design but consisting of differently sized hydrogel chambers ($Ø_1 = 3$ mm and $Ø_2 = 8$ mm) are used to investigate tube formation, vessel length, and area covered throughout the hydrogel in the presence of growth factor gradients. Figure 2 shows the impact of growth factor depletion on vascular network formation caused by diffusion-distance limitation and the elution of molecules produced by stem cells as well as endothelial cells during medium replacement. Results shown in Fig. 2(a) and supplementary material Fig. 3 revealed that vascular network formation occurred homogeneously throughout the smaller cultivation chamber ($Ø_1 = 3$ mm, $V = 7.5\,\mu$l), covering approximately 9% of the entire growth volume with 15–20 junctions per mm^2. Since the average vessel length increased from $297 \pm 26\,\mu$m within the first 1 mm to 439 ± 60 over a 3 mm distance into the cultivation chambers, sufficient supply of nutrients is provided throughout the whole cultivation chamber. In turn, results shown in Fig. 2(b) point at the presence of a biochemical gradient, since vascular network parameters varied greatly throughout the 8 mm long ($V = 100\,\mu$l) fibrin hydrogel construct. Within the first 3 mm distance from the medium supply channel, peak values for vessel area coverage of $40.4 \pm 5.9\%$, an average vessel length of 2.05 ± 0.94 mm and 22 ± 2 junctions per mm^2 are found. Between 3 and 8 mm distance, however, the quality of pre-vascular network formation declined gradually resulting in an average reduction in vessel area of $2.5 \pm 2.2\%$, a vessel length of 0.18 ± 0.25 mm and of 2.19 ± 0.1 junctions per mm^2.

To gain a better understanding of the underlying mechanisms responsible for the distance-dependent decline in the quality of pre-vascular network, fluorescently labelled dextran similar in size as proangiogenic molecules including a 10 kDa dextran (e.g., EGF and IGF), a 20 kDa dextran (e.g., ß-FGF and PDGF), and a 40 kDa dextran (e.g., VEGF and Ang-1/-2) as well as FITC-dextran with 500 kDa in size was chosen as a reference molecule to visualize gradient formation inside the fibrin hydrogel constructs under static conditions; for representative images of the dextran diffusion and a comparison of *in vitro* to *in silico* results, see supplementary material Figs. 4 and 5. Based on these results, finite volume CFD simulations were performed to determine the distribution of differently sized biomolecules inside the hydrogel volume. Figure 3(a) shows that approximately 30% of proangiogenic biomolecules with 40 kDa in size and 50% of smaller molecules are readily delivered within 12 h to cells residing up to 3 mm inside the hydrogel construct (for three dimensional graphs see also supplementary material Fig. 6). This is followed by the formation of a steep gradient starting around 3 mm hydrogel distance where only 10% of 20 kDa biomolecules but hardly any 40 kDa sized proangiogenic

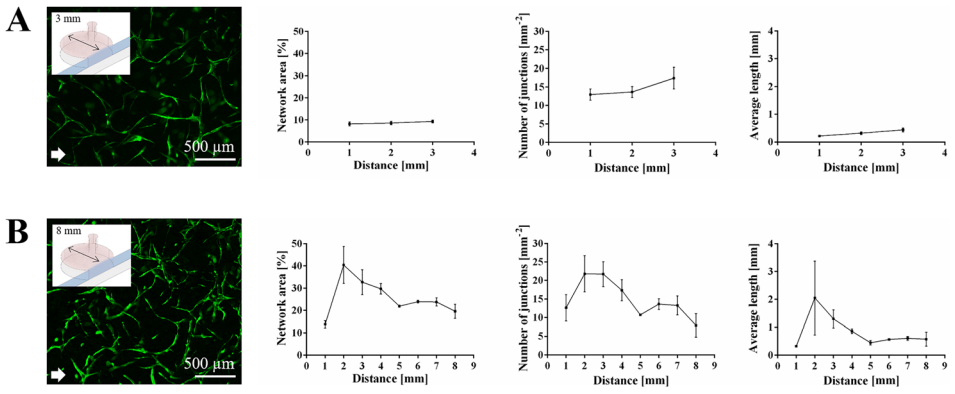

FIG. 2. Fluorescence images of pre-vascular networks with quality parameters in fibrin-based hydrogel constructs seeded with adipose-derived stem cells and green-fluorescent endothelial cells for (a) 3 mm and (b) 8 mm hydrogel chamber diameter day 7 post seeding.

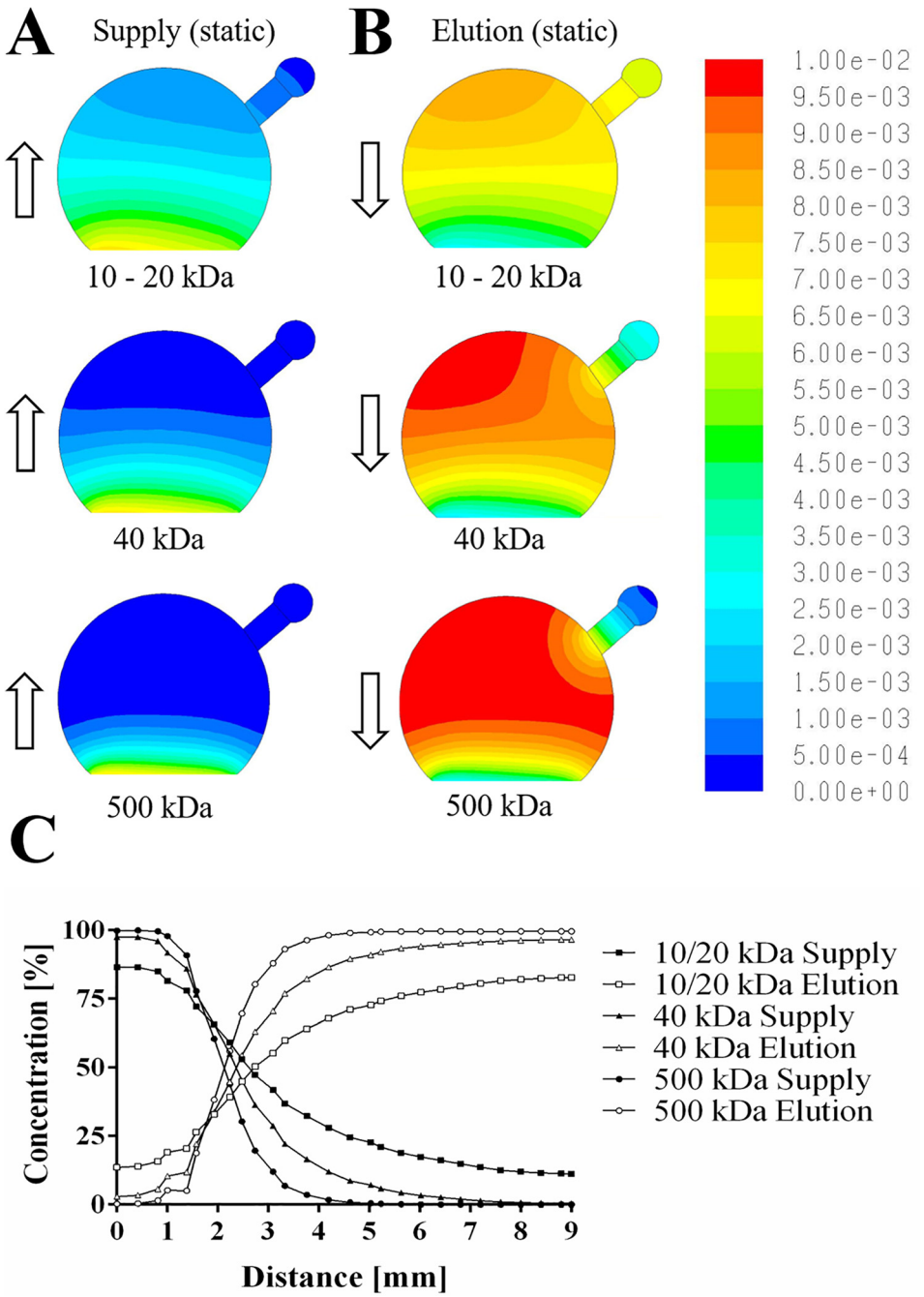

FIG. 3. Finite volume CFD simulations of size-dependent molecule diffusion (a) and elution (b) for static cell culture conditions and (c) concentration profile of molecules with distance.

factors can reach deeper regions of the fibrin hydrogel. Any larger biomolecules only diffuse up to a distance of 2 mm reaching approximately 5% of mass after a 12 h period. Additionally, the removal of secreted biomolecules and elution into the medium supply channel was simulated to estimate the distribution of cell signaling molecules within the fibrin hydrogel construct. Results shown in Fig. 3(b) indicate that over 80% of secreted biomolecules are eluted from the first millimeter and 50% are still eluted from up to 3 mm inside the fibrin construct. In other words, small hydrogel volumes are prone to elution of proangiogenic factors, thus severely impeding reciprocal cell-cell signaling events.

Overall, our simulation results correlate well with experimental differences observed in vascular network formation using microfluidic co-cultures of adipose-derived stem cells with endothelial cells, indicating that distance between 2 to 3 mm inside the hydrogel reaches optimum equilibrium between nutrient supply and elution of metabolites for pre-vascular network formation in static culture conditions. Since the 8 mm diameter hydrogel chamber design displayed gradient-dependent network formation, it was selected for subsequent flow experiments.

Impact of direct and indirect interstitial fluid flow on pre-vascular network formation

In addition to diffusion-limited supply of nutrients, interstitial flow conditions can also influence vascular network formation due to the increased elution of secreted biomolecules. To study the effects of direct and indirect fluid flow on pre-vascular network formation, two different microfluidic geometries shown in Fig. 4 are employed in subsequent experiments. In the first microfluidic configuration (right panel of Fig. 4) indirect interstitial flow conditions are established by directing the medium flow alongside the hydrogel interface at a velocity of 3 μm/s, whereas the second microchip design (left panel of Fig. 4) was adjusted to reduce hydrogel resistance and increase hydrogel anchorage to enable direct flow through the hydrogel. Results of our lateral flow direction study revealed that microfluidic ASCs/HUVEC co-cultures embedded in 8 mm fibrin hydrogel constructs started to form vascular connections already at day 3. Since apparent vascular network morphologies improved over the following 4 days in culture, sufficient supply of reciprocal signaling of proangiogenic growth factors is provided during indirect medium perfusion. In contrast, fluid flow forced through the fibrin hydrogel

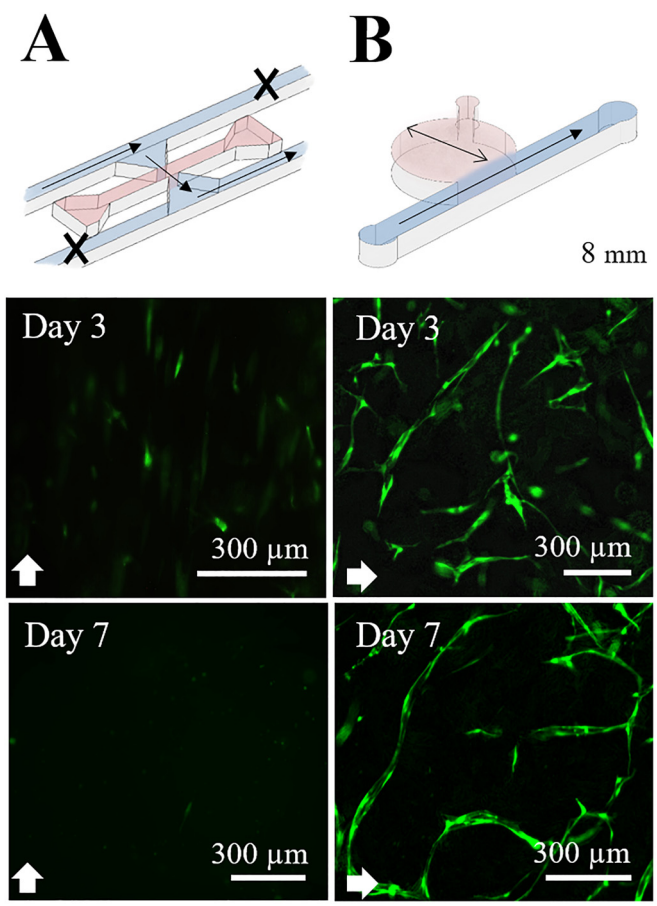

FIG. 4. Influence of direct compared to orthogonal interstitial fluid flow on pre-vascular network formation.

construct using our second microfluidic configuration (left panel of Fig. 4) resulted in endothelial cell alignment in the direction of the fluid flow with no evidence of pre-vascular network formation at day 3. Even more striking, complete loss of endothelial cell viability occurred by day 7 under direct interstitial fluid flow conditions. Additionally, finite volume CFD simulations (see supplementary video 1) revealed that direct fluid flow through a hydrogel results in complete elution of pro-angiogenic growth factors from the perfused region already after 120 s, thus eliminating reciprocal cell signaling and the formation of vascular structures. In other words, secretion of proangiogenic growth factors from the adipose-derived stem cells plays a key role in the initial phase of vascular network formation, while forced fluid flow through a hydrogel construct may be beneficial in maturation of preformed lumenized vessels.

Interstitial flow enhances sprouting but lessens network maturation

Since reciprocal cell-cell signaling is an important part during the onset and formation of pre-vascular networks, additional finite volume CFD simulations were performed to assess the distribution of proangiogenic growth factors in fibrin hydrogel constructs. *In silico* results shown in Fig. 5 indicate that during indirect lateral flow conditions sufficient growth factors are present over the complete hydrogel distance, where 50% of 20 kDa sized molecules reach 4 mm and 40% diffuse up to 6 mm into the hydrogel within a period of 12 h. Additionally, Fig. 5(a) shows that approximately 50% of biomolecules ranging from 10 to 20 kDa in size are delivered in a similarly fashion to static cultures. It is important to note, however, that slightly higher biomolecule concentrations in the deeper regions of the hydrogel construct could be achieved in the presence of lateral fluid flow. Interestingly, lateral fluid flow did not increase the penetration depth of 40 and 500 kDa biomolecules after 12 h of perfusion. Furthermore, elution of proangiogenic growth factors from the fibrin hydrogel construct is significantly enhanced for smaller biomolecules sizes with complete removal from the first millimeter distance [see Fig. 5(b)], while bigger sized molecules displayed similar distribution as static cultivation.

In a next set of experiments, network area coverage, vessel length, and number of junctions of microfluidic *in vitro* co-cultures of stem cells and endothelial cells were evaluated to assess the quality of vascular network formation in the presence of physiologically relevant fluid flow rates that resemble interstitial flow regimes. Figure 6(a) shows a cross-section analysis of the 3D-cultivation chambers where images of endothelial tube formation are compared, revealing good agreement with above *in silico* results. While endothelial cell alignment along the flow direction is found within the first millimeter where highest flow rates are present, premature vascular connections started to form 2 mm inside the hydrogel exhibiting a vessel area coverage of $5.11 \pm 1.42\%$, 51 ± 12 junctions mm^{-2}, and an average vessel length of 0.066 ± 0.008 mm. In turn, within deeper regions around 4 mm inside of the hydrogel construct, vascular network formation improved markedly featuring a vessel area of $12.07 \pm 1.21\%$, 155 ± 16 junctions mm^{-2}, and an average vessel length of 0.16 ± 0.02 mm. This improved vascular structure quality suggests efficient nutrient delivery to the entire hydrogel volume, while simultaneously retaining secreted cell signaling molecules, thus promoting homogenous vascular network formation.

In a final comparative analysis, vascular network formation in the presence of varying concentration gradients was investigated to assess the impact of size-depended growth factor distribution inside the hydrogel construct. Additionally, we investigated whether preconditioning of culture medium in stem cell secretome or application of a stop-flow regime alters vascular network formation. Results of our comparative study are summarized in Fig. 7 where size-dependent biomolecule distribution and vascular network formation of ASC and HUVEC co-cultures embedded in fibrin hydrogels are analyzed. Results in Fig. 7(a) illustrate that the distribution of biomolecules in the range of 10 and 20 kDa differs between 20% to 40% over a distance of 1, 3, and 6 mm inside the hydrogel construct in the presence of indirect perfusion. These phenomena can mainly be attributed to the elution and removal of smaller molecules from the hydrogel during lateral flow conditions. The evaluation of the quality of the vascular structures over the distance in the absence and presence of interstitial flow is shown in

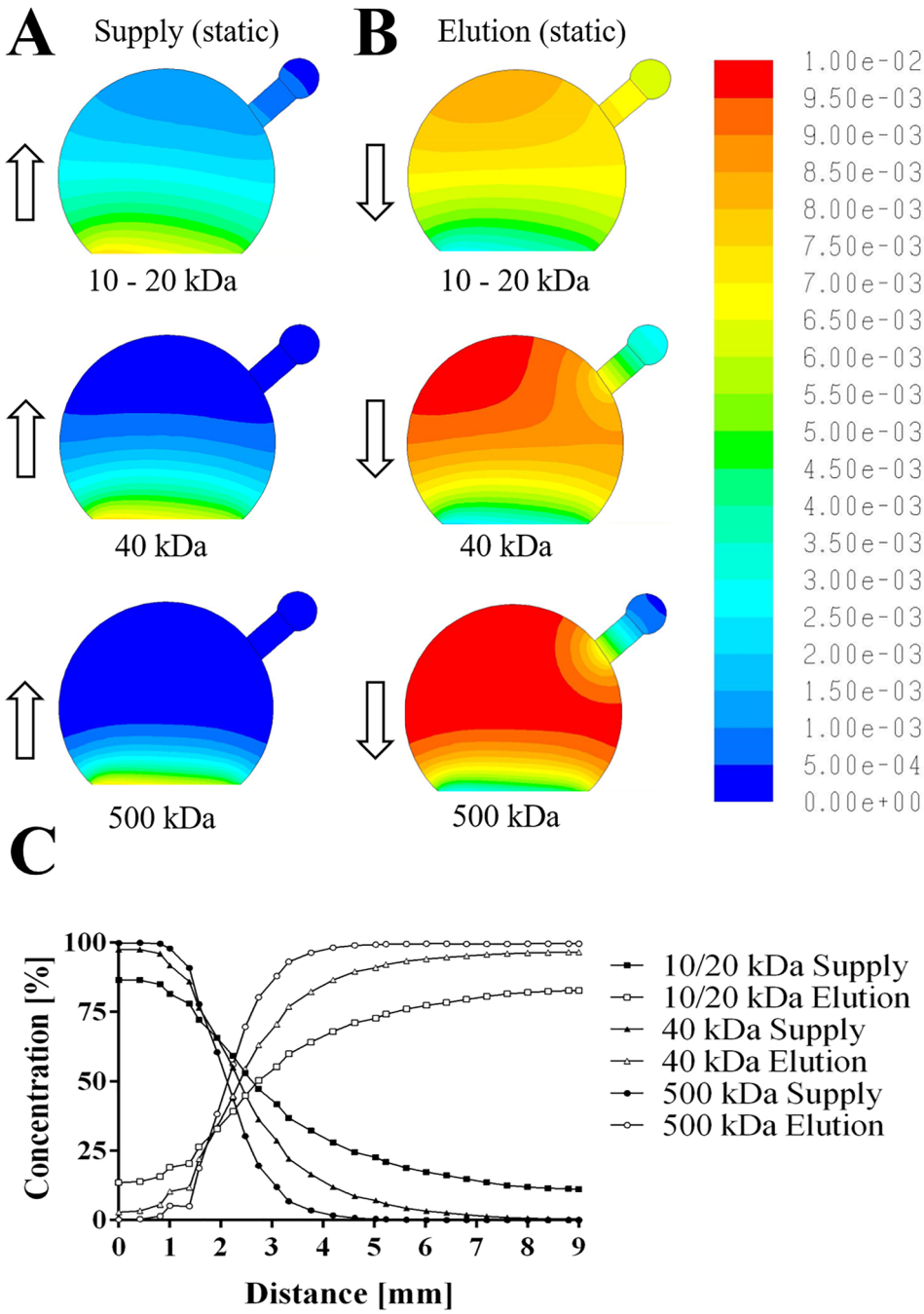

FIG. 5. Finite volume CFD simulations of size-dependent molecule diffusion (a) and elution (b) for indirect interstitial fluid flow and (c) concentration profile of molecules with distance.

Fig. 7(b). While lateral perfusion of the fibrin-hydrogel construct led to improved endothelial sprouting events, reduced vessel length and network area coverage, particularly inside deeper regions (< 4 mm), are found compared to static conditions. Although dynamic culture conditions resulted in overall lower vascular network quality values, the obtained vascular morphology displayed a higher degree uniformity and regularity throughout the fibrin hydrogel construct. These results point at the mitigating effect of local concentration of proangiogenic biomolecules, which is governed by supply of nutrients, maintenance of secretome, and elution of metabolic waste products. In a final set of experiments, we investigated the possibility to

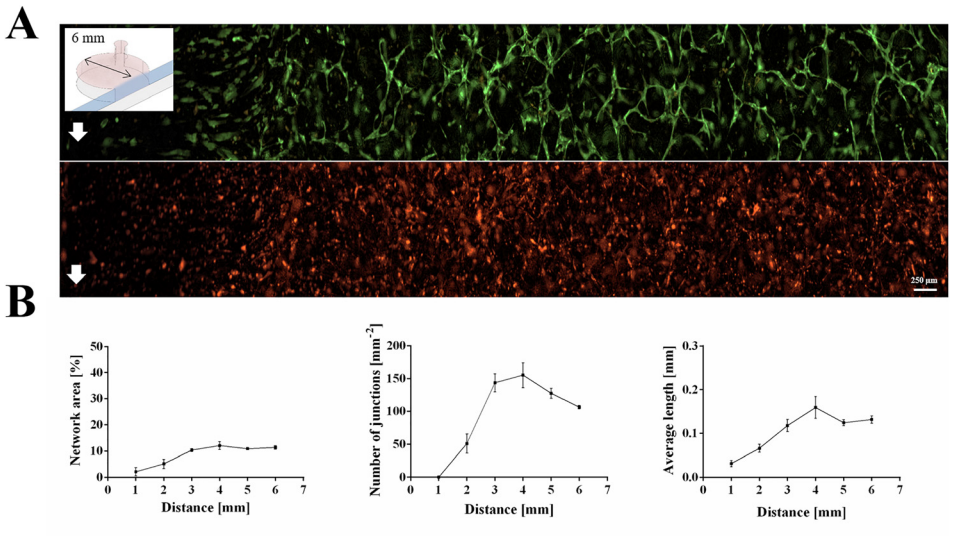

FIG. 6. (a) Fluorescence images pre-vascular networks and (b) quality parameters of adipose-derived stem cells (red) and umbilical vein endothelial cells (green) at interstitial fluid flow day 7 post seeding.

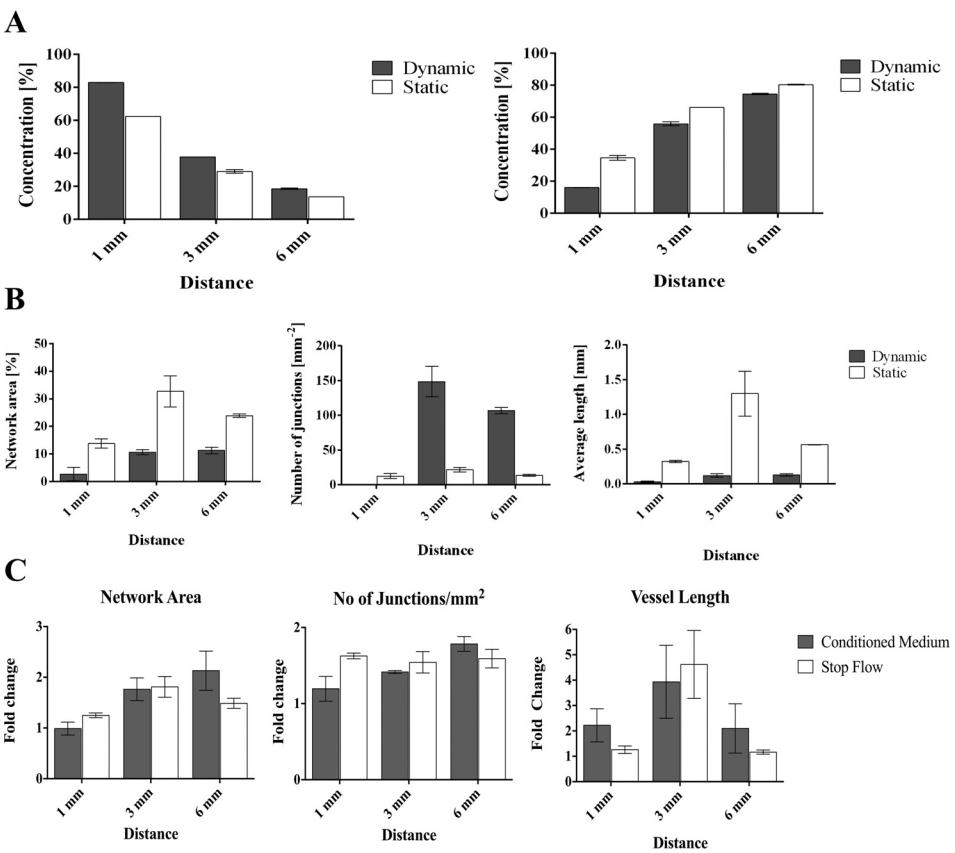

FIG. 7. (a) Finite volume CFD simulations of biomolecule diffusion in static compared to dynamic cell culture conditions. (b) Comparison of pre-vascular network formation for static and dynamic culture conditions using microfluidic devices day 7 post seeding. (c) Fold changes of network characteristics during cultivation with ASC conditioned medium (grey) and temporal adjustment of flow regime (white) compared to the initial flow setup.

improve vessel parameters by either employing a setup with temporal adjustment of flow or stem cell conditioned culture medium in the initial setup in the presence of continuous flow directly after cell seeding. In the "temporal adjustment of flow setup" (Stop-Flow), the co-cultures were cultivated statically for three days to allow establishment of preliminary vascular connections before application of flow for the final five days of culture. Results of both setups are displayed in Fig. 7(c) and show a minor improvement of network area and number of junctions/mm^2 within the first millimeter of the construct. However, both parameters were visibly increased at distances of 3 and 6 mm into the construct. Interestingly, temporal adjustment of flow resulted in 4.6-times longer vessels at 3 mm from the medium channel but only slight improvement at the other distances while the stem cell conditioned medium enhanced the vessel length at all distances.

CONCLUSION

In this work, we have investigated the influence of concentration gradients on the formation of vascular networks inside fibrin-hydrogel constructs containing human umbilical vein endothelial cells and adipose-derived stem cells. Using three different microfluidic 3D vascular co-culture models, the importance of biochemical gradients and reciprocal cell signaling events on endothelial sprouting was demonstrated in the absence and presence of indirect as well as direct flow conditions. Starting with single elongated cells at the edges of the hydrogel construct, pre-vascular network formation started within 0.5–1 mm distance inside the fibrin hydrogel for all devices. In the absence of fluid flow, pre-vascular microvessels formation occurred predominantly inside 2–3 mm inside the fibrin construct followed by subsequent decline of vascular network quality. The observed asymmetry in endothelial sprouting events can be attributed to diffusional transport limitations of nutrients into deeper zones of the vascular co-culture model. In turn, direct perfusion through the fibrin construct resulted in endothelial cell alignment in flow direction during the first three days of culture; however, no tube formation was obtained after 7 days. Indirect perfusion based on the lateral flow direction showed significantly higher sprouting activity and uniformity throughout the hydrogel construct, but also exhibited a reduced vascular network area coverage and decreased average microvessel length. To gain deeper insights into gradient-mediated endothelial sprouting within a 3D matrix, an *in silico* assessment of size-dependent biomolecule distribution was performed. Our finite volume CFD simulations are based on experimental data derived from differently sized and fluorescently labeled dextrans. The selected size range of 10, 20, 40, and 500 kDa soluble molecules correspond to the size of major signaling molecules and growth factors present during vascular network formation. Results from the finite volume CFD simulations on the distribution profiles of differently sized proangiogenic molecules suggest that at least a 1:1 ratio between fresh nutrient supply and elution of reciprocal signaling molecules, produced locally within the hydrogel construct by the co-culture, is best suited to ensure efficient vascular network formation. This ratio corresponds to a balance of delivery of 50% fresh medium supplements and retention of 50% of reciprocal signaling molecules inside the fibrin hydrogel, a comparative graph of supply and elution in both static and dynamic conditions can be found in Fig. 7(a). In summary, we found that the establishment of growth factor gradients via lateral fluid flow on the order of micrometers per second enhances endothelial cell sprouting and heterotypic cell-cell interactions facilitate initial network formation. However, after vessel maturation, spatio-temporal control of direct perfusion in microvascular systems is of utmost importance to ensure proper endothelial phenotype. In other words, direct flow through a hydrogel construct is only beneficial in the presence of mature lumenized microvessels, since adipose-derived stem cell secretome plays a key role in the initial phase of vascular network formation.

SUPPLEMENTARY MATERIAL

See supplementary material for additional information on microchip geometries, finite volume CFD simulations, and FITC-dextran diffusion experiments.

ACKNOWLEDGMENTS

This work was funded by the European Union's INTERREG V-A AT-CZ programme (ATCZ133), the European Union's Horizon 2020 research and innovation programme (685817), the City of Vienna Tissue Engineering International Project (MA 23, #14–06), and the Austrian Research Promotion Agency (FFG; 849791). The authors also thank Carina Huber-Gries for fruitful discussions.

[1]R. Costa-Almeida, P. L. Granja, R. Soares, and S. G. Guerreiro, Eur. Cell Mater. **28**, 51–66 (2014).
[2]M. Lovett, K. Lee, A. Edwards, and D. L. Kaplan, Tissue Eng. Part B, Rev. **15**(3), 353–370 (2009).
[3]E. A. Phelps and A. J. Garcia, Curr. Opin. Biotechnol. **21**(5), 704–709 (2010).
[4]G. D. Yancopoulos, S. Davis, N. W. Gale, J. S. Rudge, S. J. Wiegand, and J. Holash, Nature **407**(6801), 242–248 (2000).
[5]W. Risau, Nature **386**(6626), 671–674 (1997).
[6]K. Pill, S. Hofmann, H. Redl, and W. Holnthoner, Cell Regener. (Lond) **4**, 8 (2015).
[7]K. Gaengel, G. Genove, A. Armulik, and C. Betsholtz, Arterioscler., Thromb., Vasc. Biol. **29**(5), 630–638 (2009).
[8]F. Verseijden, S. J. Posthumus-van Sluijs, P. Pavljasevic, S. O. Hofer, G. J. van Osch, and E. Farrell, Tissue Eng. Part A **16**(1), 101–114 (2010).
[9]S. Merfeld-Clauss, N. Gollahalli, K. L. March, and D. O. Traktuev, Tissue Eng. Part A **16**(9), 2953–2966 (2010).
[10]J. Rehman, D. Traktuev, J. Li, S. Merfeld-Clauss, C. J. Temm-Grove, J. E. Bovenkerk, C. L. Pell, B. H. Johnstone, R. V. Considine, and K. L. March, Circulation **109**(10), 1292–1298 (2004).
[11]S. Rohringer, P. Hofbauer, K. H. Schneider, A. M. Husa, G. Feichtinger, A. Peterbauer-Scherb, H. Redl, and W. Holnthoner, Angiogenesis **17**(4), 921–933 (2014).
[12]D. Wartmann, M. Rothbauer, O. Kuten, C. Barresi, C. Visus, T. Felzmann, and P. Ertl, Front. Mater. **2**, 60 (2015).
[13]D. Sticker, S. Lechner, C. Jungreuthmayer, J. Zanghellini, and P. Ertl, Anal. Chem. **89**(4), 2326–2333 (2017).
[14]M. Rothbauer, H. Zirath, and P. Ertl, Lab Chip **18**(2), 249–270 (2018).
[15]M. Rothbauer, D. Wartmann, V. Charwat, and P. Ertl, Biotechnol. Adv. **33**(6 Pt 1), 948–961 (2015).
[16]M. Rothbauer, I. Praisler, D. Docter, R. H. Stauber, and P. Ertl, Biosensors (Basel) **5**(4), 736–749 (2015).
[17]J. M. Rosser, I. Olmos-Calvo, M. Schlager, M. Purtscher, F. Jenner, and P. Ertl, J. Cell Biol. Cell Metab. **2**, 005 (2015).
[18]K. Aizel, A. G. Clark, A. Simon, S. Geraldo, A. Funfak, P. Vargas, J. Bibette, D. M. Vignjevic, and N. Bremond, Lab Chip **17**(22), 3851–3861 (2017).
[19]I. K. Zervantonakis, S. K. Hughes-Alford, J. L. Charest, J. S. Condeelis, F. B. Gertler, and R. D. Kamm, Proc. Natl. Acad. Sci. U. S. A. **109**(34), 13515–13520 (2012).
[20]J. S. Jeon, S. Bersini, M. Gilardi, G. Dubini, J. L. Charest, M. Moretti, and R. D. Kamm, Proc. Natl. Acad. Sci. U. S. A. **112**(1), 214–219 (2015).
[21]Y. Shin, J. S. Jeon, S. Han, G. S. Jung, S. Shin, S. H. Lee, R. Sudo, R. D. Kamm, and S. Chung, Lab Chip **11**(13), 2175–2181 (2011).
[22]W. A. Farahat, L. B. Wood, I. K. Zervantonakis, A. Schor, S. Ong, D. Neal, R. D. Kamm, and H. H. Asada, PLoS One **7**(5), e37333 (2012).
[23]J. W. Song and L. L. Munn, Proc. Natl. Acad. Sci. U. S. A. **108**(37), 15342–15347 (2011).
[24]C. L. Helm, M. E. Fleury, A. H. Zisch, F. Boschetti, and M. A. Swartz, Proc. Natl. Acad. Sci. U. S. A. **102**(44), 15779–15784 (2005).
[25]K. Haase and R. D. Kamm, Regener. Med. **12**(3), 285–302 (2017).
[26]Q. Smith and S. Gerecht, Curr. Opin. Chem. Eng. **3**, 42–50 (2014).
[27]Y. H. Hsu, M. L. Moya, C. C. Hughes, S. C. George, and A. P. Lee, Lab Chip **13**(15), 2990–2998 (2013).
[28]C. Bonvin, J. Overney, A. C. Shieh, J. B. Dixon, and M. A. Swartz, Biotechnol. Bioeng. **105**(5), 982–991 (2010).
[29]J. S. Jeon, S. Bersini, J. A. Whisler, M. B. Chen, G. Dubini, J. L. Charest, M. Moretti, and R. D. Kamm, Integr. Biol. (Camb) **6**(5), 555–563 (2014).
[30]S. Kim, H. Lee, M. Chung, and N. L. Jeon, Lab Chip **13**(8), 1489–1500 (2013).
[31]A. Sobrino, D. T. T. Phan, R. Datta, X. Wang, S. J. Hachey, M. Romero-López, E. Gratton, A. P. Lee, S. C. George, and C. C. W. Hughes, Sci. Rep. **6**, 31589 (2016).
[32]W. J. Polacheck, M. L. Kutys, J. Yang, J. Eyckmans, Y. Wu, H. Vasavada, K. K. Hirschi, and C. S. Chen, Nature **552**, 258 (2017).
[33]S. Wolbank, A. Peterbauer, M. Fahrner, S. Hennerbichler, M. van Griensven, G. Stadler, H. Redl, and C. Gabriel, Tissue Eng. **13**(6), 1173–1183 (2007).
[34]P. Petzelbauer, J. R. Bender, J. Wilson, and J. S. Pober, J. Immunol. **151**(9), 5062–5072 (1993), available at https://www.ncbi.nlm.nih.gov/pubmed/7691964.
[35]S. Muhleder, K. Pill, M. Schaupper, K. Labuda, E. Priglinger, P. Hofbauer, V. Charwat, U. Marx, H. Redl, and W. Holnthoner, Stem Cell Res. Ther. **9**(1), 35 (2018).
[36]L. Knezevic, M. Schaupper, S. Muhleder, K. Schimek, T. Hasenberg, U. Marx, E. Priglinger, H. Redl, and W. Holnthoner, Front. Bioeng. Biotechnol. **5**, 25 (2017).
[37]E. Zudaire, L. Gambardella, C. Kurcz, and S. Vermeren, PLoS One **6**(11), e27385 (2011).